Nitric acid in the middle stratosphere as a function of altitude and aerosol loading

K. W. Jucks, D. G. Johnson, K. V. Chance, and W. A. Traub
Harvard-Smithsonian Center for Astrophysics, Cambridge, Massachusetts

R. J. Salawitch
Jet Propulsion Laboratory, Pasadena, California

Abstract

We present remote-sensing measurements of the abundance of nitric acid (HNO_3) in the lower and middle stratosphere (between 16 and 40 km) covering the period 1989–1997. The measurements were made with the Smithsonian Astrophysical Observatory Far-Infrared Spectrometer (FIRS-2) under a wide range of aerosol surface area density. We compare our measurements with the results of a photochemical steady state model to test our understanding of the chemistry of HNO_3 under a variety of conditions. We find that HNO_3 is significantly overestimated by the model at altitudes above 22 km, with the difference increasing with increasing altitude and decreasing aerosol surface area density. The agreement between modeled and measured HNO_3 can be improved by either decreasing the rate of $\mathrm{OH} + \mathrm{NO_2}$ by 35% or by using newly measured rate constants for the reactions $\mathrm{OH} + \mathrm{NO_2}$ and $\mathrm{OH} + \mathrm{HNO_3}$, but significant differences remain. We discuss these observations in the context of possible uncertainties in the calculated photolysis rate of HNO_3 at wavelengths near 200 nm, uncertainties in the observations, errors caused by the use of constrained steady state models, and possible missing sink reactions for HNO_3.

1. Introduction

Understanding the partitioning of reactive nitrogen compounds in the stratosphere is important for a number of reasons. Catalytic cycles involving NO and NO_2 regulate the abundance of ozone in the middle stratosphere (22–40 km), so accurate modeling of ozone loss requires a good understanding of the partitioning of nitrogen compounds between radicals (NO and NO_2) and reservoirs (HNO_3, N_2O_5, $ClNO_3$, and HNO_4). Also, levels of NO and NO_2 help control the partitioning of inorganic chlorine compounds and of OH and HO_2, all of which affect the photochemical balance of ozone. We define here the quantities $[NO_x]$ and $[NO_y]$, where $[\mathrm{NO}_x] = [\mathrm{NO}] + [\mathrm{NO}_2] + [\mathrm{NO}_3]$, $[\mathrm{NO}_y] = [\mathrm{NO}_x] + [\mathrm{HNO}_3] + 2[\mathrm{N}_2\mathrm{O}_5] + [\mathrm{ClNO}_3] + [\mathrm{HNO}_4] + [\mathrm{HNO}_2] + [\mathrm{BrNO}_3]$, and $[X]$ denotes the volume mixing ratio of X. Most of NO_y below 30 km is in the form of HNO_3. The primary reactions that convert NO_x to HNO_3 are

$$\mathrm{OH} + \mathrm{NO_2} + \mathrm{M} \rightarrow \mathrm{HNO_3} \tag{1}$$

and the heterogeneous reactions on liquid sulfate aerosols

$$\mathrm{N_2O_5} + \mathrm{H_2O} \rightarrow 2\mathrm{HNO_3}\,, \tag{2}$$

$$\mathrm{BrNO_3} + \mathrm{H_2O} \rightarrow \mathrm{HNO_3} + \mathrm{HOBr}\,, \tag{3}$$

$$\mathrm{ClNO_3} + \mathrm{H_2O} \rightarrow \mathrm{HNO_3} + \mathrm{HOCl}\,, \tag{4}$$

where N_2O_5, $BrNO_3$, and $ClNO_3$ are formed by reactions of NO_2 with radicals. The dominant NO_y reservoir, HNO_3 is converted back to NO_x either by photolysis,

$$\mathrm{HNO_3} + \mathrm{h}\nu \rightarrow \mathrm{NO_2} + \mathrm{OH} \tag{5}$$

or by the reaction

$$\mathrm{HNO_3} + \mathrm{OH} \rightarrow \mathrm{NO_3} + \mathrm{H_2O}. \tag{6}$$

In addition, each of the less abundant NO_y reservoir species (N_2O_5, $BrNO_3$, and $ClNO_3$) can photolyze to produce NO_2.

Recent studies of NO_y partitioning show that [NO], $[NO_2]$, and $[NO_x]/[NO_y]$ are well modeled in the stratosphere below 20 km under conditions of moderate to relatively high aerosol loading [*Gao et al.*, 1997]. However, *Sen et al.* [1998] find that a model using recommended rates and cross sections [*DeMore et al.*, 1994] significantly underestimates $[NO_x]/[NO_y]$ at higher altitudes, especially during conditions of low-aerosol loading. Similar conclusions were reached by the analysis of $[NO_x]/[NO_y]$ measured by instruments aboard the UARS satellite [*Morris et al.*, 1997; *Danilin et al.*, 1999].

In the present study we explore the partitioning of NO_y in the stratosphere by comparing Smithsonian Astrophysical Observatory Far-Infrared Spectrometer (FIRS-2) measurements of $[HNO_3]$ with the results of numerous photochemical simulations for various assumptions regarding key kinetic parameters. The model is constrained by FIRS-2 measurements of temperature, $[O_3]$, $[H_2O]$, and $[N_2O]$ (used to estimate $[NO_y]$, $[Cl_y]$, $[Br_y]$, and $[CH_4]$). The validity of each simulation is tested further by comparing model calculations with FIRS-2 measurements of [OH], $[HO_2]$, $[NO_2]$, $[N_2O_5]$, and $[ClNO_3]$. We use data from one balloon flight on April 30, 1997, near Fairbanks, Alaska (68°N, 149°W), together with data from six northern hemisphere midlatitude flights which took place between 1989 and 1994. These observations cover a wide range of aerosol loading and solar illumination. We use these observations to show that concentrations of HNO_3 in the middle stratosphere are systematically overestimated by photochemical model calculations. The magnitude of this discrepancy is greatest for the observations with the lowest aerosol loading in which case the production of HNO_3 is driven primarily by reaction (1). We also show that the discrepancy between observed and calculated $[HNO_3]$ cannot be completely resolved by an adjustment to the rate of reaction (1) or by the use of recently measured rates for reactions (1) and (6). We conclude part of the discrepancy may result from the model undercalculating the photolysis rate of HNO_3 at wavelengths near 200 nm.

2. Measurements

The FIRS-2 is a remote-sensing Fourier transform spectrometer that operates mostly from balloon platforms [*Johnson et al.*, 1995a]. The spectrometer measures atmospheric thermal emission in the band 75–1300 cm^{-1}, producing spectra that are used to retrieve simultaneous concentration profiles for 28 different molecules, including OH, HO_2, H_2O_2, NO_2, HNO_3, HNO_4, N_2O_5, HCl, HOCl, $ClNO_3$, N_2O, O_3, H_2O, and CH_4. Improvements to the instrument before the last balloon flight from Fairbanks allowed for the retrievals of profiles from shorter wavelength bands for CH_4, HNO_4, and N_2O_5 which were not available from the previous flights. For daytime flights we can estimate [ClO] from measurements of [HOCl], $[HO_2]$, and [OH] [*Johnson et al.*, 1995b], and [NO] from measurements of [OH], $[HO_2]$, and $[O_3]$ since the partitioning between OH and HO_2 is driven primarily by NO and O_3. The uncertainties in inferred [NO] are fairly large owing to the large uncertainties in the rate of OH+O_3. The derivation of [NO] breaks down above 35 km where atomic O starts to dominate HO_x partitioning [*Jucks et*

al., 1998]. The group of molecules measured by FIRS-2 forms a comprehensive set for examining stratospheric photochemistry [*Chance et al.*, 1996; *Jucks et al.*, 1996, 1998, also unpublished manuscript, 1999].

Spectra are obtained at a series of regularly spaced tangent heights below the balloon during both day and night. The retrieval algorithm has been described in detail elsewhere [*Johnson et al.*, 1995a, 1996; *Jucks et al.*, 1998]. Data presented here were obtained during balloon flights launched on September 24, 1989, June 5, 1990, May 29, 1992, September 29, 1992, March 23, 1993, May 22, 1994, and April 30, 1997. All but the last flight provided observation footprints at latitudes between 30° and 38°N. The latter flight, launched from Fairbanks, Alaska, provided observations near 68°N. The combined data set provides concentration profiles for a wide range of aerosol loading and solar illumination.

The spectroscopic transitions used for most molecules and the spectroscopic errors associated with those transitions are discussed by *Jucks et al.* [1998], *Johnson et al.*, [1996], and *Chance et al.* [1996]; the discussion here will be limited to HNO_3, N_2O, and O_3. The profile of $[HNO_3]$ is retrieved from the ν_9 band centered near 458 cm^{-1}. This is a strong vibrational band with very few spectral interferences from other molecules, and the precision in the lower and middle stratosphere is better than 0.2 ppb for most of the data presented here. The absolute accuracy is 10% due to the large uncertainties in the absolute strengths for all bands of HNO_3 [*Goldman et al.*, 1998; *Perrin*, 1998]. For the 1997 flight we were able to retrieve concentrations of HNO_3 using the $\nu_5/2\nu_9$ bands (one of the bands used by solar occultation instruments) in addition to the ν_9 band. We find that concentrations retrieved using the $\nu_5/2\nu_9$ are 8±3% lower than those from the ν_9 band. Most of this difference can be attributed to the uncertainties in the absolute strengths of these two bands.

For flights prior to 1997, we retrieve $[O_3]$ using only far-infrared rotational transitions. These transitions become obscured in the lower stratosphere, limiting the precision below 20 km. For the 1997 flight we are able to use mid-infrared ν_2 transitions in addition to the pure rotational transitions greatly improving the measurement precision below 22 km.

$[N_2O]$ is retrieved from more than 20 P and R branch transitions of the ν_2 band (centered near 588 cm^{-1}) using the parameters from *Johns et al.* [1996]. The strengths of the transitions are measured to better than 2% [*Johns et al.*, 1996].

All error bars shown in the figures discussed in this study include all the random errors associated with the retrievals of the concentrations. These errors include the uncertainties in the retrievals from random noise in the spectra, uncertainties from errors in the observational geometry, spectrum normalization errors, and temperature errors. Systematic uncertainties resulting from uncertainties in the spectroscopic constants used for the retrievals are not included. These uncertainties are discussed below as they relate to the analysis.

3. Models

We use a photochemical steady state model that is constrained by temperature, $[H_2O]$, $[O_3]$, $[CH_4]$, $[NO_y]$, $[Cl_y]$, $[Br_y]$, and aerosol surface area [*Salawitch et al.*, 1994]. The model inputs are either directly measured by the FIRS-2 or derived from FIRS-2 measurements using established tracer correlations described below. We use FIRS-2 measurements of temperature, $[H_2O]$, and $[O_3]$. For data sets obtained before 1997, the precision of the $[O_3]$ profiles below 22 km is poor, and when available we use the profile of $[O_3]$ obtained on ascent by the JPL *in situ* UV photometer for altitudes below 22 km. The FIRS-2 and *in situ* profiles of $[O_3]$ show good agreement above 22 km. Since $[CH_4]$ is only retrieved for the Fairbanks flight, we derive $[CH_4]$ from FIRS-2 $[N_2O]$ using relationships derived from Atmospheric Trace MOlecule Spectroscopy Experiment (ATMOS) observations [*Michelsen et al.*, 1998a] for the midlatitude flights. Uncertainties in the $[CH_4]$ model constraint have only a small effect on calculated partitioning of NO_y species since CH_4 is a minor source of HO_x. The profile of $[Cl_y]$ is estimated from FIRS-2 $[N_2O]$ using the relationship derived by *Woodbridge et al.* [1995]. The estimated $[Cl_y]$ agrees well with FIRS-2 measurements of $[Cl_y]$ and $[N_2O]$ in 1994 and 1997, where measured $[Cl_y]$ is approximated by $[HCl] + [ClNO_3] + [HOCl] + [ClO]$ [K. W. Jucks et al., unpublished manuscript, 1999]. $[Br_y]$ is also estimated from $[N_2O]$, with a maximum value of 21 pptv. Profiles of aerosol surface area are based on zonal monthly mean measurements obtained by Stratospheric Aerosol and Gas Experiment (SAGE II) [*Thomason et al.*, 1997]. The variability of aerosol surface area around the zonal mean value ranges from 20 to 40% between 20 and 30 km at northern midlatitudes.

We estimate $[NO_y]$ from both $[N_2O]$ and $[O_3]$ using relationships derived from ATMOS observations [*Michelsen et al.*, 1998b]. We use the O_3 relation in the lower stratosphere (which is similar to the midlatitude relationships derived from *in situ* observations by *Volk et al.* [1996]) because the *in situ* observations of $[O_3]$ yield a more precise estimate of $[NO_y]$ at low altitude than the FIRS-2 measurements of $[N_2O]$. We use the N_2O relation in the

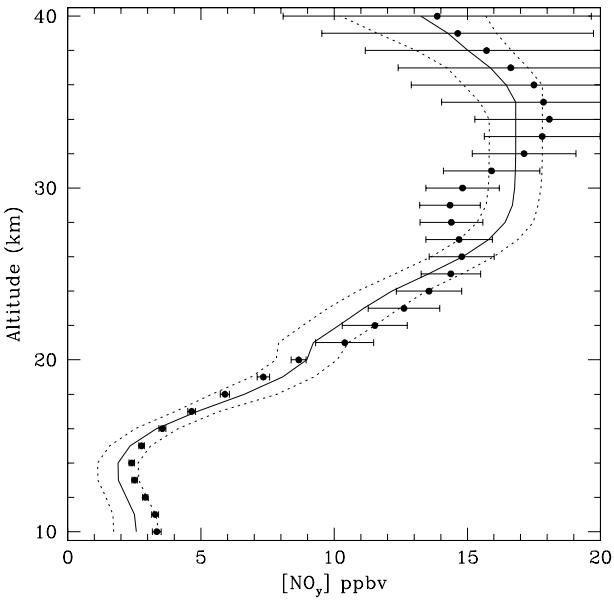

Figure 1. Comparison of measured and estimated [NO_y]. Measured [NO_y] (solid circles) is calculated from FIRS-2 measurements of [HNO_3], [NO_2], [$ClNO_3$], [N_2O_5], and [NO] (inferred from measurements of [OH], [HO_2], and [O_3]) from the balloon flight on April 30, 1997 near 68°N. Modeled [NO_y] (solid curve) is estimated from FIRS-2 measurements of [O_3] below 20 km, and from measurements of [N_2O] above 20 km, using relationships derived from midlatitude ATMOS observations [*Michelsen et al.*, 1998b]. The 1σ uncertainty in estimated [NO_y] is indicated by the dotted lines.

middle stratosphere (generally above 24 km, depending on the flight) since the correlation of [O_3] and [NO_y] breaks down in this region. We show a comparison of estimated and measured [NO_y] in Figure 1. The data are from the 1997 balloon flight, the only flight where all the individual constituents of NO_y were observed. The measured [NO_y] is given by $[HNO_3] + [HNO_4] + [ClNO_3] + 2[N_2O_5] + [NO_2] + [NO]^*$, where $[NO]^*$ has been derived from measured [OH], [HO_2], and [O_3]. The species that are normally used in the definition of NO_y but are not measured by FIRS-2, such as $BrNO_3$, HNO_2, and NO_3, are estimated to make a negligible contribution to the NO_y budget. The 1σ uncertainties in the inferred [NO_y] reflect the uncertainties in observed [O_3] and [N_2O] projected into the relationships and the uncertainties in the ATMOS observations of [NO_y] used to derive the relationships. The estimated and measured [NO_y] show good agreement, even though the observations were made at a higher latitude than the observations used to develop the NO_y versus N_2O and NO_y versus O_3 relationships.

We have run three versions of our photochemical model for the present analysis. The models use reaction rates, cross sections, and heterogeneous reaction probabilities based on the recommendations of *DeMore et al.* [1997], with slight modifications. Models A, B, and C include a 7% branching ratio for ClO+OH→HCl+O_2 as suggested by laboratory measurements [*Lipson et al.*, 1997] and atmospheric observations [*Chance et al.*, 1996; *Michelsen et al.*, 1996]. Model B includes 25% reductions in the rates of $OH + HO_2$ and $O + HO_2$, which improves the agreement with FIRS-2 observations of [HO_2] [*Jucks et al.*, 1998], as well as a 35% reduction in the rate of $OH + NO_2$ as used in a previous study [*Osterman et al.*, 1999]. Model C includes the reduction in the rates of the HO_2 reactions as well as recently measured rates for $OH + NO_2$ and $OH + HNO_3$ [*Dransfield et al.*, 1999; *Brown et al.*, 1999]. The slower rate for the reaction O+NO_2 measured by *Brown et al.* [1999] has little affect on NO_x or NO_y partitioning since this reaction is slow compared to NO_2 photolysis. However, this reaction does significantly affect the calculated loss rate of ozone since it is the rate-limiting step for an important odd oxygen catalytic loss cycle. The change in the rates of the HO_2 reactions has little effect on the calculated NO_y partitioning because the calculated OH profile is not significantly changed.

4. Comparison of Models and Measurements

Several recent studies of NO_y partitioning have found significant differences between calculations and measurements, particularly for conditions when reaction (1) is the dominant NO_x sink. *In situ* measurements of [NO_x]/[NO_y] in the lower stratosphere during the Photochemistry of Ozone Loss in the Arctic Region in Summer (POLARIS) campaign at high latitudes during summer exceed calculated values by 38% [*Gao et al.*, 1999], whereas the observations obtained during the higher-aerosol conditions of earlier campaigns showed good agreement with calculations [*Gao et al.*, 1997]. Studies of balloon-borne solar occultation measurements in the lower and middle stratosphere have reached similar conclusions [*Sen et al.*, 1998; *Osterman et al.*, 1999].

Recent laboratory kinetics data suggest that the rate of reaction (1) may be slower than the currently recommended rate [*DeMore et al.*,1997] by roughly 20% to 25% for typical temperatures and pressures in the lower stratosphere and roughly 30% near 30 km [*Dransfield et al.*, 1999; *Brown et al.*, 1999] and that the rate of reaction (6)

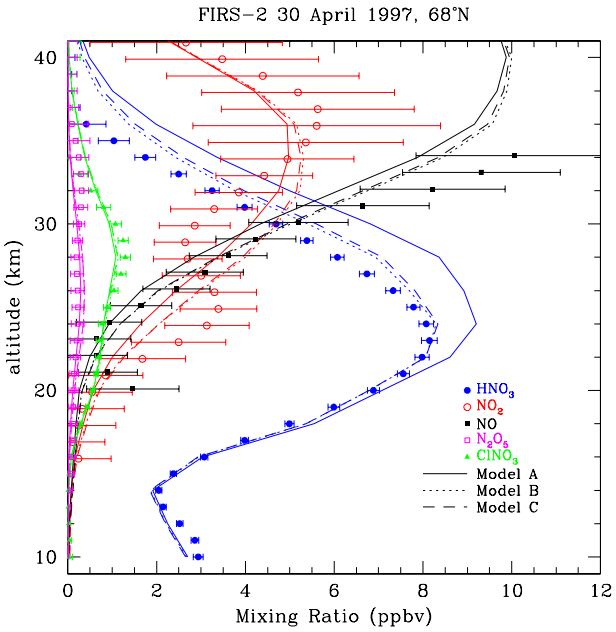

Plate 1. Observed and modeled [HNO_3], [NO_2], [$ClNO_3$], [N_2O_5], and [NO] (derived from the relationship described in the text) from the FIRS-2 balloon flight on April 30, 1997, near 68°N. Models A, B, and C are described in the text. All measurement error bars contain the compilation of all random errors affecting concentration retrievals, but not systematic errors from uncertainties in spectroscopic parameters used.

may be up to 120% faster than the current recommendation [*Brown et al.*, 1999]. *Osterman et al.* [1999] find that the solar occultation observations of NO_y partitioning obtained by MkIV during POLARIS are in good agreement with a model in which the rate of reaction (1) has been reduced by 35% (a change similar to what was suggested by the recent laboratory measurements), while *Gao et al.* [1999] found that a model including the newly measured rates for reactions (1) and (6) still undercalculated [NO_x]/[NO_y] by 10% near 20 km.

We show in Plate 1 a comparison of models A, B, and C with FIRS-2 observations of [HNO_3], [NO_2], [$ClNO_3$], [N_2O_5], and estimated [NO] near Fairbanks, Alaska, on April 30, 1997. The uncertainties in estimated [NO] are dominated by the uncertainty at stratospheric temperatures in the rates of HO_2+NO (20%) and OH+O_3 (40%). Models B and C give similar results to each other (suggesting that the model used by *Osterman et al.* [1999] and *Gao et al.* [1999] should be similar) and are in better agreement with the data than model A, but all models overestimate [HNO_3] above 25 km. We note that model B is similar to a model which was found to agree well with MkIV observations of [NO], [NO_2], [N_2O_5], and [HNO_3] at the same latitude in May and July [*Osterman et al.*, 1999].

Most of the differences in the conclusions between our results from the April 30, 1997, flight and that from the MkIV data (which was taken 8 days later at similar latitudes) results from differences in transport history of the air masses sampled. The profiles of [HNO_3] from the two instruments agree within the uncertainties, and the MkIV summed [NO_y] agrees with the [NO_y] inferred from N_2O used here. Similar good agreement for HNO_3 and NO_y (as well as O_3) was seen when FIRS-2 and MkIV flew on the same gondola at mid latitudes in 1994. The MkIV profile of [O_3] is consistently lower than the FIRS-2 values between 22 and 32 km by roughly 1 ppm, suggesting considerably different types of air masses. The model constrained with the MkIV [O_3] will calculate a slower rate for reaction (1) since there will be less calculated [OH] and a faster rate for reaction (5) since less UV flux is absorbed than the modeled constrained with the FIRS-2 [O_3]. An *in situ* UV photometer on board the gondola with FIRS-2 obtained concentrations of [O_3] that agree with the FIRS-2 data to within the uncertainties [*Jucks et al.*. 1998, Figure 1]. Similar agreement between [O_3] from the MkIV and *in situ* data also has been shown [*Sen et al.*, 1998]. We do not believe that systematic errors in the retrieved [O_3] exist for either of these data sets and that the differences in the observed [O_3] result from differences in the observed air masses.

Back trajectory calculations support the assumption of different air masses. The photochemical lifetimes of HNO_3 are of the order of 2 days (at 32 km) to 15 days (at 24 km), and the ratio of [HNO_3]/[NO_y] is lower for lower latitudes due to faster photolysis rates for HNO_3. Between 20 and 32 km, most of the air masses sampled by FIRS-2 were at latitudes 10° to 20° south of the measurement location over the past 10 days, while for the MkIV observations, most of the air was on average 5° to 10° to the north of the observation latitudes (R. Kawa, private communications, 1998). If the transport histories were to be taken into account, then the FIRS-2 data would agree somewhat better, while the MkIV data would show less good agreement with the model B, with both models similarly underestimating the observed [NO_x]/[NO_y].

In Figure 2 we compare measured and modeled [HNO_3] on June 6, 1990, May 29, 1992, and May 22, 1994. We show data from high (May 1992), moderate (May 1994), and low (June 1990) aerosol periods. The aerosol loading in 1990 and 1997 are similar. Models B and C overestimate [HNO_3] above 25 km for the low

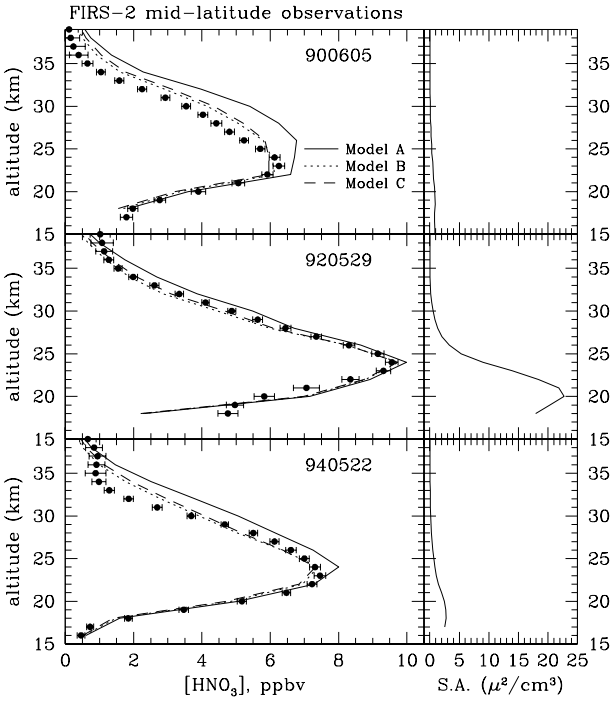

Figure 2. Comparison of modeled [HNO_3] with FIRS-2 measurements from flights near 35°N before, during, and shortly after the peak of aerosol loading from Mount Pinatubo. The right panels show the SAGE II zonal monthly mean surface areas for each of these flights. The models are the same as in Plate 1.

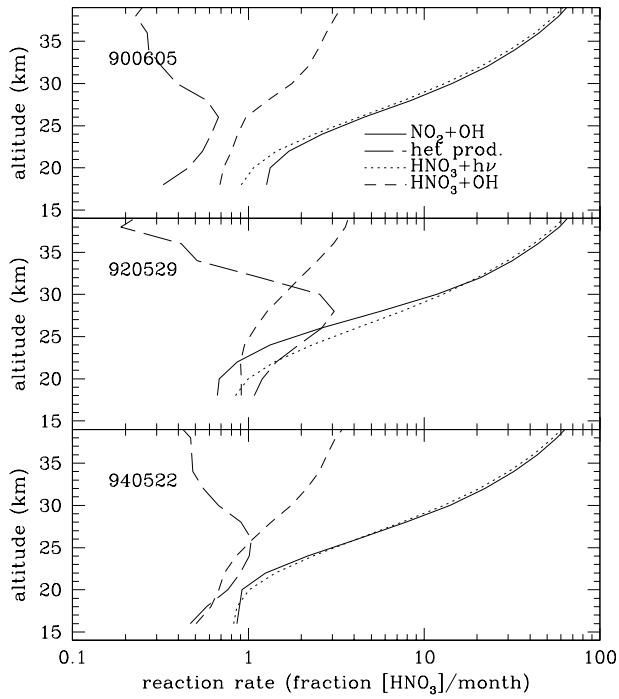

Figure 3. Calculated rates for the reactions which dominate production and loss of HNO_3 for three flights with different aerosol loading. The heterogeneous production curve is the sum of the production of HNO_3 from N_2O_5 hydrolysis, $BrNO_3$ hydrolysis, and a minor contribution from $ClNO_3$ hydrolysis. All of these models correspond to data taken near 37°N.

and moderate aerosol cases, but these simulations agree well with the measurements of [HNO_3] made during the high-aerosol period in 1992. Model A is also in better agreement with the measurements of [HNO_3] made in 1992 than with observations obtained at other times. The comparisons for September 1992 (not shown), also a period of high aerosol concentration, are similar to the results for May 1992. Our conclusion that the best agreement between modeled and measured NO_y partitioning is obtained during times of high aerosol loading is consistent with the conclusions of *Gao et al.* [1997] and *Sen et al.* [1998]. All these flights were taken at the spring stratospheric wind turnaround at midlatitudes where the latitude gradient in photolysis rate of HNO_3 will be much less than that for the high-latitude data. Thus errors from the assumption of a single latitude in the steady state model are not as significant as for the data shown in Plate 1.

Figure 3 shows calculated rates of the reactions controlling the abundance of HNO_3 for the flights of June 90, May 1992, and May 1994. All rates were found using model A. Reaction (1) is the primary source of HNO_3 at nearly all altitudes for low to moderate aerosol concentrations, while the heterogeneous reactions (3) and (4) dominate production of HNO_3 in the lower stratosphere at high aerosol concentrations. For the high aerosol conditions of the May 1992 flight the heterogeneous reactions dominate production of HNO_3 up to 26 km, above which reaction (1) dominates. The crossover point drops to 23 km for the September 29, 1992 flight (not shown), resulting from a subsidence of the aerosol layer between the two flights. The relative importance of reaction (1) and the heterogeneous reactions is similar for all low-aerosol flights.

Photolysis is the dominant sink of HNO_3 for all FIRS-2 flights, especially above 20 km. The main difference between flights in the relative contributions of photolysis and reaction (6) to the loss of HNO_3 is that the contribution of reaction (6) peaks at higher altitudes (near 30 km) for the high-latitude flight (not shown) than for the midlatitude

flights.

The combined FIRS-2 data set samples a wide range of altitudes and aerosol loading and thus a wide range of relative contributions of reactions (1)–(6) to production and loss of HNO_3. To compare models and measurements for all flights within a coherent framework we have adopted a "chemical coordinate system" first suggested by (R. C. Cohen, manuscript in preparation, 1999]. This formalism examines the ratio of measured to modeled concentration of a particular species as a function of the relative contribution of a specific reaction to the total production or loss of that species. A systematic error in the calculated rate of one reaction will result in a systematic change in the ratio of the measured to modeled concentration as a function of the relative importance of that reaction. For the data presented here, the ratio of measured to modeled $[HNO_3]$ is plotted against the relative contributions of reactions (1) or (5) to the production or loss of HNO_3. The remainder of the production of HNO_3 is from the sums of the heterogeneous reactions, while the remainder of the loss of is due to reaction (6).

Plate 2 shows the ratio of measured to modeled $[HNO_3]$ as a function of both the relative contribution of reaction (1) to total production of HNO_3 (the sum of reactions (1) through (4)) and the relative contribution of reaction (5) to total loss of HNO_3 (reactions (5) and (6)). The estimated errors include both the uncertainty in measured $[HNO_3]$ and the uncertainty in modeled $[HNO_3]$ resulting from the estimated error in the inferred $[NO_y]$. Because the coordinates are model-dependent, we show separate plots for models A, B, and C. We only show data for altitudes between 20 and 34 km. The relative error in the $[HNO_3]$ measurements increases rapidly above 34 km, and HNO_3 is no longer a sensitive probe of NO_y partitioning below 20 km since $[HNO_3]/[NO_y] \approx 1$ in the lower stratosphere.

The ratio of measured to modeled $[HNO_3]$ shown in Plate 2 is less than 1.0 when either the production is dominated by reaction (1) or the loss is dominated by reaction (5). This is generally the case for the data at higher altitudes as shown in Figure 3. Models B and C are in better agreement with the data than model A (as already shown in Plate 1 and Figure 2), but significant differences remain. The ratio of measured to modeled $[HNO_3]$ shows considerable curvature when plotted against the production coordinate (left panels in Plate 2), particularly when reaction (1) accounts for more than 80% of total production, while the behavior is more linear when the ratio is plotted against the loss coordinate (right panels in Plate 2).

A number of systematic errors may affect this analysis, including the assumption of a single latitude for the

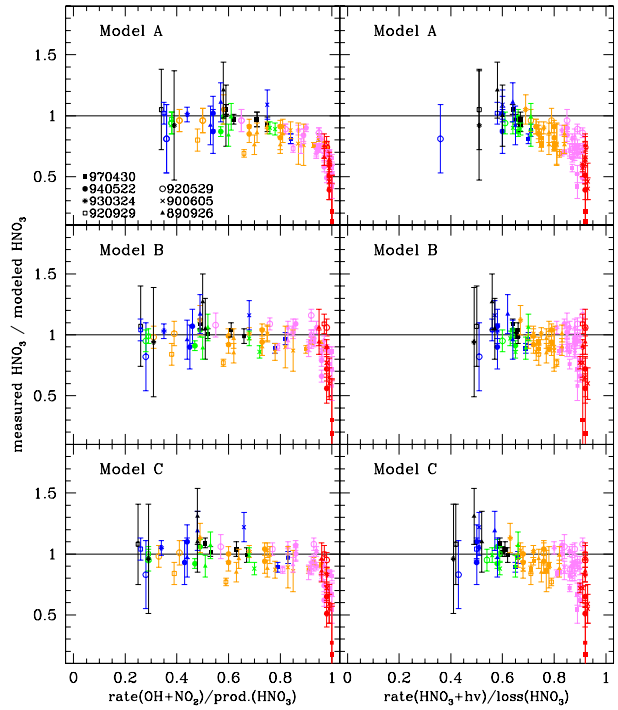

Plate 2. Ratio of measured to modeled $[HNO_3]$ for seven flights of the FIRS-2 spectrometer for all three models as a function of calculated relative contribution to production (left panels) and loss (right panels) of HNO_3. The error bars contain all random uncertainties in the retrievals of $[HNO_3]$ and uncertainties in the retrieved N_2O projected into the modeled $[HNO_3]$. The color coding of the data points indicates the modeled contribution to photolysis of HNO_3 from absorption between 190 and 230 nm: black is <20%, blue is 20% to 40%, green is 40% to 60%, orange is 60% to 80%, pink is 80% to 90%, and red is >90%.

steady state calculations discussed above. We note that the estimated uncertainty in the HNO_3 line strengths is 10% [*Goldman et al.*, 1998; *Perrin*, 1998], resulting in a 10% uncertainty in the retrieved HNO_3 abundance. An error in the line strengths would result in a uniform vertical offset for all the data in Plate 2. The measurement precision is included in the error bars.

Estimating $[NO_y]$ from measured $[N_2O]$ introduces another source of error. Note that model to measurement comparisons shown in Plate 2 do not include the altitude range for which the O_3 correlation is used to infer $[NO_y]$. The uncertainty in the midlatitude $[NO_y]$-$[N_2O]$ relationship derived from ATMOS measurements is estimated to be 15% [*Michelsen et al.*, 1998b], based on the

estimated error for measurements of individual species. These uncertainties, along with the uncertainties in measured [N_2O] reflected into the relationship, are included in the error bars in Plate 2. The estimated error varies depending on which molecules dominate NO_y at a particular altitude. The ATMOS midlatitude relationship agrees well with FIRS-2 observations from the high-latitude flight in April 1997, as shown in Figure 1. This flight occurred well outside the arctic vortex, prior to the final warming, thus we did not observe any vortex-like filaments in tracer-tracer relationships. The [NO_y]-[N_2O] relationship used here also agrees with ER-2 based *in situ* measurements to within 13% [*Chang et al.*, 1996] and within the uncertainties of the [NO_y]-[N_2O] obtained from the MkIV data used by *Osterman et al.* [1999]. We conclude that the error in estimated [NO_y] is not large enough to account for the difference between measured and modeled [HNO_3].

The model calculations are affected by errors in the SAGE II aerosol surface area densities, particularly at the altitudes where the heterogeneous reactions significantly affect NO_y partitioning (Figure 3). The assumptions used to convert the SAGE II extinction to aerosol surface area density are discussed by *Thomason et al.* [1997]. We note that errors in surface area will have the largest effect on calculations where the surface areas are at moderate levels (in the lower stratosphere for the flights with the lowest surface areas and in the middle stratosphere for flights with the highest surface areas) because the rate of the most dominant heterogeneous source of HNO_3 (reaction (2)) saturates at high surface areas.

As seen in Plate 1 and Figure 2, the discrepancy between measured and calculated [HNO_3] is greatest for the data at higher altitudes and low surface areas, where the heterogeneous reactions are not a significant source of HNO_3. This is illustrated in Plate 2 by the fact that the data from the high-aerosol flights in 1992 (the open circles and squares) have measured to modeled ratios much closer to 1.0 than the other flights. It is not possible to decrease the heterogeneous production of HNO_3 for the low-aerosol data sets enough to make the comparison between measured and modeled [HNO_3] consistent to the high-aerosol data. This suggests that their is a potential problem with the gas phase destruction of HNO_3. On the other hand, if such a correction were made to all the data sets presented here such that the low aerosol data agreed with the model (see discussion below), then the models would significantly underpredict the observations above 22 km for the higher-aerosol data sets. We are using zonal monthly mean surface areas which may vary from the local surface areas by as much as 50%. If all our data during the high aerosol time periods were made when the local concentrations were higher than the zonal mean values, then the calculated rate of the heterogeneous reactions would be biased low, and calculated [HNO_3] would be systematically low. Another possible source of error in the calculated heterogeneous rates is the lack of temperature and size distribution sensitivity for the calculation of the uptake coefficient for reaction (2).

The model simulations of [HNO_3] are dependent on calculated [OH], since OH participates in production (reaction (1)) and loss (reaction (6)) of HNO_3. Calculations of [OH] with model A agree well with measurements of [OH] obtained by FIRS-2 [*Jucks et al.*, 1998] and appear to underestimate ER-2 based *in situ* observations of OH by 10 to 15% [*Salawitch et al.*, 1994]. Calculations of [OH] with a model including the same changes to the HO_2 reactions as models B and C agree as well as model A with measured [OH], and agree with measured [HO_2] more closely than model A calculations [*Jucks et al.*, 1998].

Another possible source of error in the model is the calculation of the photolysis rate of HNO_3 (reaction (5)). This calculation depends on the measured altitude profile for [O_3], the solar irradiance model, accurate representation of the absorption of UV radiation by O_2 and O_3, and accurate UV absorption cross sections for HNO_3. The altitude profile of [O_3] is measured for each of these data sets with the same set of spectra used in this study and has an accuracy of better than 10% for all data sets. For a few of these data sets, we validated the measured [O_3] with concentrations measured by an *in situ* photometer and found agreement with FIRS-2 profiles to within its uncertainties (J. Margitan, private communications, 1998]. As stated above, errors in [O_3] used to constrain the model will have two effects on the partitioning of NO_y; it will affect the calculated photolysis rate of HNO_3, and it will affect the calculated [HO_x] which in turn affects the rates of reactions (1) and (6).

The HNO_3 cross sections used in our model [*Burkholder et al.*, 1993] agree well with previous measurements at wavelengths less than 300 nm, but differ significantly at longer wavelengths where interferences from NO_2 become important. Most of the HNO_3 photolysis in the lower stratosphere results from absorption at wavelengths greater than 290 nm, where the cross section is decreasing with increasing wavelength. In the middle and upper stratosphere, at altitudes greater than 24 km, significant absorption occurs at shorter wavelengths (centered near 200 nm) where the HNO_3 cross section is considerably larger [*Burkholder et al.*, 1993, Figure 10]. The photolysis code used for calculating the photolysis rates is summarized by *Minschwaner et al.* [1993] where it was shown to agree with atmospheric transmission data to

within 20%. The solar irradiance model is taken from the 1985 World Meteorological Organization (WMO) assessment and agrees with most recent measurements of solar irradiance as a function of frequency to within 10%.

5. Discussion

Our conclusion that a standard photochemical model (model A) overestimates [HNO_3] and therefore underestimates [NO_x]/[NO_y] is consistent with the results of *Gao et al.* [1999] and *Osterman et al.* [1999]. The result that model C, which used recent laboratory measurements for rate of OH+NO_2+M (reaction (1)) and OH+HNO_3 (reaction (6)), overestimates [HNO_3] during periods of low-aerosol abundance is consistent with the study of *Gao et al.* [1999], who find that a model similar to our model C underestimates [NO_x]/[NO_y] for *in situ* data obtained during the POLARIS mission. Unlike *Osterman et al.* [1999], we find that a 35% reduction in the rate of reaction (1) (model B) is not sufficient to match the observations of [HNO_3] above 25 km (Plate 1 and Figure 3). As mentioned above, this is most likely due to lack of consideration for the latitude history of the air masses by the constrained steady state model used both in this study and by *Osterman et al.* [1999] . This, along with uncertainties in the local aerosol surface areas mentioned above, could account for most of the spread in the data plotted in Plate 2. We have not obtained back trajectory calculations for the midlatitude data sets as most of these data were taken during stratospheric wind turnaround times when the uncertainties in back trajectory analyses are high.

Assuming that the latitude histories for the midlatitude are consistent with the observation latitudes over a period of 5 to 10 days, further changes to the rate constant of reaction (1) will not resolve the discrepancy between measured and calculated HNO_3 shown here without increasing the negative temperature dependence of this reaction by an unrealistic amount. Even including the 35% reduction in the rate of OH+NO_2 used by *Osterman et al.* [1999], a change only slightly larger than suggested by recent laboratory measurements [*Dransfield et al.*, 1999; *Brown et al.*, 1999], does not produce agreement with the FIRS-2 measurements of [HNO_3] when reaction (1) accounts for more than 90% of the total production of HNO_3. Changing the rate constant without changing the temperature dependence will effectively change the slope of the ratios in Plate 2 and not change the curvature in the relationship. The fact that the ratio of measured to modeled [HNO_3] shows considerable curvature when plotted against the relative OH+NO_2 production coordinate in Plate 2 (left panels) suggests that either there is a missing loss reaction of HNO_3 which dominates where reaction (1) is the dominant production channel (generally above 25 km) and is not significant elsewhere, or there are problems with the calculation of the primary loss processes. We again note that systematic errors in measured [HNO_3] or inferred [NO_y] will not add significant slope or curvature to the relations in Plate 2, and will instead cause a vertical shift of the data.

The ratio of the relative contribution of photolysis to total loss (right panels) appears to be a linear as a function of total photolysis, with the difference between measured and modeled [HNO_3] increasing with increasing importance (especially for the lower-aerosol flights before and after 1992) of photolysis and not the curved relationship seen relative to the OH+NO_2 coordinate. This indicates that there may be an error in the calculated photolysis rates and not reaction (6) since a change in the rate constant in reaction (6) would not affect the ratios of measured to modeled [HNO_3] where the discrepancy is greatest. A simple scaling of the photolysis rate by an amount sufficient to resolve the discrepancy for the data where photolysis dominates loss of HNO_3 would overcorrect the data where photolysis has less importance by an amount consistent with the uncertainties in the measurements since the ratios of measured to modeled [HNO_3] is effectively 1.0 for the points where photolysis contributes about 50% of the loss of HNO_3. However, the wavelengths which are most important for HNO_3 photolysis have a distinct altitude dependence, as shown by *Burkholder et al.* [1993, Figure 10]. Most of the photolysis of HNO_3 above 24 km occurs in a 30 nm wide band centered around 200 nm, whereas below this altitude photolysis from wavelengths between 290 and 330 nm dominates. This is the same altitude dependence as seen for the difference between measured and calculated [HNO_3] (Plate 1 and Figure 2), suggesting that an error in the calculated photolysis rates near 200 nm could be an explanation for the discrepancy. This is illustrated by the color coding in Plate 2. The red points are those where 90% or more of the photolysis of HNO_3 comes from near 200 nm, while the black points are from those points where less than 20% of the photolysis comes from wavelengths near 200 nm. There is a clear separation between the different color bands as a function of percentage of the total loss of HNO_3 due to photolysis (as expected), and there is a systematic increase in the discrepancy in the ratio of measured to modeled [HNO_3] with increase in the percentage of photolysis near 200 nm.

Other possible HNO_3 loss channels, such as reactions with atomic O or Cl, are included in this model and have been measured to be orders of magnitude too slow to affect NO_y partitioning and so are unlikely causes of the differ-

ence between calculated and observed [HNO_3]. The reaction rate constant of HNO_3 with $O(^1D)$ has not been measured, but if one assumes it proceeds with the same rate constant as the reaction of $O(^1D)$ and H_2O, then it would still be several orders of magnitude slower than the photolysis rate at all altitudes in the stratosphere. Other such undocumented reactions with HNO_3 may be important, with the most likely candidates to consider are reactions with radicals (like Br) that have concentrations which increase with increasing altitude.

Potential uncertainties in the calculated photolysis rates were discussed above, but specific points are addressed here for completeness. One possible source of error is an uncertainty in the HNO_3 absorption cross section at wavelengths near 200 nm. However, cross sections in this wavelength range have been measured by many groups and all agree to within 20% [*Burkholder et al.*, 1993], which is much smaller than the 60% needed to completely reconcile the discrepancies seen in Plate 1. Somewhat smaller changes can reconcile the other flights. We consider it unlikely that all these laboratory measurements are in error by such a large amount.

Another possibility is an underestimation of the UV flux near 200 nm by the model. This could result from overestimating the overhead ozone column, underestimating the solar flux at short wavelengths, or an error in the algorithm used to calculate UV absorption by O_2 and O_3. The overhead O_3 column is measured with a total uncertainty of less than 10% for all data sets. The solar flux spectrum used in the model is adapted from WMO [1986]. The variation over a solar cycle in solar flux near 200 nm is only $\pm 5\%$ and agrees with recent measurements to better than 10% [*Lean et al.*, 1997, 1992], making uncertainties in solar input an unlikely source of significant error in calculated photolysis of HNO_3. Increasing the flux by 60% at wavelengths shorter than 240 nm gives similar agreement to the data in Plate 1 to that obtained for a 60% change in the cross sections of HNO_3. Again, this change is much larger than can be justified from solar irradiance measurements.

Proper radiative transfer near 200 nm relies on using proper parameterization for the Schumann-Runge bands and Herzberg continuum of O_2 and the short wavelength side of the O_3 Hartley band, both of which are derived from recent measurements and validated against measured atmospheric transmissions (see *Minschwaner et al.* [1993] for details). The algorithm we use for absorption by O_2 has also been compared to the results of a line-by-line calculation and is accurate to within 10% [*Minschwaner et al.*, 1993].

A total uncertainty of 50% in the calculated photolysis rate (cross section (20%) + solar irradiance (10%) + algorithm (10%) + [O_3] profile (10%)), combined with a 10% systematic error in measured [HNO_3] and the roughly 10% random retrieval uncertainty in the ratio of measured to modeled [HNO_3] (which includes the uncertainty in modeled [NO_y]) would be enough to account for the observations, but they would have to all sum up in the same direction which is unlikely. Because the individual estimated uncertainties in the calculated photolysis rate are small relative to the observed discrepancy, we cannot recommend photolysis as a singular cause of the discrepancy. Plus, changes to the model to increase the UV flux could also affect the calculation of [$O(^3P)$], [$O(^1D)$], O_2 photolysis rates, and calculated stratospheric lifetimes of long-lived tracers like N_2O and CFCs, depending on the particular changes made.

The data clearly show a discrepancy between measured and modeled [HNO_3] using the currently recommended rates and cross sections, which is reduced but not eliminated by the use of more recent kinetics measurements. At present, we cannot identify a single source of error which can account for the remaining difference between calculated and measured [HNO_3] above 22 km using the recently recommended rates for reactions (1) and (6), although errors in the calculated short-wavelength photolysis rate, errors in calculated [HNO_3]/[NO_y] from assumption of constant latitude during the steady state model calculation, and a potential missing loss reaction for HNO_3 remain open possibilities which merit future investigation given the implications.

Acknowledgments We wish to thank the Japanese Space Agency (NASDA) for funding the flight from Fairbanks, Alaska, as part of the ADEOS Alaska validation campaign and the NASA Upper Atmosphere Research Program for funding the midlatitude flights, four of which were part of the UARS correlative program. We are grateful to the Jet Propulsion Laboratory Atmospheric Ballooning group for gondola support and to the National Scientific Balloon Facility for launch services. We thank Jim Margitan for use of his O_3 data that was used as a model constraint for some of the balloon flights. We thank Neil Donahue, Steve Brown, Greg Osterman, Ru-Shan Gao, Ron Cohen, and Hope Michelsen for providing us with their preliminary results prior to publication. All of these data were very helpful to this investigation. We thank Randy Kawa of NASA Goddard for the back trajectory calculations of the data taken during the POLARIS time frame. The work at SAO was supported by NASA grant NSG–5175. Research at the Jet Propulsion Laboratory, California Institute of Technology, was performed

under contract with NASA.

References

Brown, S. S., R. K. Talukdar, and A. R. Ravishankara, Reconsideration of the rate constant for the reaction of hydroxyl radicals with nitric acid, *J. Phys. Chem. A, 103*, 3031-3037, 1999.

Burkholder, J. B., R. K. Talukdar, A. R. Ravishankara, and S. Solomon, Temperature dependence of the HNO_3 UV absorption cross sections, *J. Geophys. Res.98*, 22937-22948, 1993.

Chance, K. V., et al., Simultaneous measurements of stratospheric HO_x, NO_x, and Cl_x: Comparison with a photochemical model, *J. Geophys. Res.101*, 9031-9043, 1996.

Chang, A. Y. et al., A comparison of measurements from ATMOS and instruments aboard the ER-2 aircraft: Tracers of atmospheric transport, *Geophys. Res. Lett.23*, 2389, 1996.

Danilin, M. Y., et al., Nitrogen species in the post-Pinatubo stratosphere: Model analysis utilizing UARS measurements, *J. Geophys. Res.104*, 8247-8262, 1999.

DeMore, W. B., et al., Chemical kinetics and photochemical data for use in stratospheric modeling: Evaluation number 11, *JPL Publ. 94-26*, 1994.

DeMore, W. B., et al., Chemical kinetics and photochemical data for use in stratospheric modeling: Evaluation number 12, *JPL Publ. 97-4*, 1997.

Donahue, N. M., M. Dubey, R. Mohrschladt, K. L. Demerjian, and J. G. Anderson, A high-pressure flow study of the reactions OH+NO_x $\rightarrow$HONO_x: Errors in the falloff region, *J. Geophys. Res.102*, 6159-6162, 1997.

Dransfield, T. J., M. M. Sprengnether, K. K. Perkins, N. M. Donahue, J. G. Anderson, and K. L. Demerjian, Temperature and pressure dependent kinetics of the gas-phase reaction of the hydroxyl radical with nitrogen dioxide, *Geophys. Res. Lett.26*, 687-690, 1999.

Gao, R. S., et al., Partitioning of the reactive nitrogen reservoir in the lower stratosphere of the southern hemisphere: Observations and modeling, *J. Geophys. Res.102*, 3935–3945, 1997.

Gao, R. S., et al., A comparison of observations and model simulations of the NO_x/NO_y ratio in the lower stratosphere, *Geophys. Res. Lett.26*, 1153-1156, 1999.

Goldman, A., C. P. Rinsland, A. Perrin, and J.-M. Flaud, HNO_3 line parameters: 1996 HITRAN update and new results, *J. Quant. Spectrosc. Radiat. Transfer, 60*, 851-861, 1998.

Johns, J. W. C., Z. Lu, M. Weber, J. M. Sirota, and D. C. Reuter, Absolute intensities in the ν_2 fundamental of N_2O at 17 μm, *J. Mol. Spectrosc., 177*, 203-210, 1996.

Johnson, D. G., K. W. Jucks, W. A. Traub, and K. V. Chance, Smithsonian stratospheric far-infrared spectrometer and data reduction system, *J. Geophys. Res.100*, 3091-3106, 1995a.

Johnson, D. G., W. A. Traub, K. V. Chance, K. W. Jucks, and R. A. Stachnik, Estimating the abundance of ClO from simultaneous remote sensing measurements of HO_2, OH, and HOCl, *Geophys. Res. Lett.22*, 1867–1871, 1995b.

Johnson, D. G., et al., Measurement of chlorine nitrate in the stratosphere using the ν_4 and ν_5 bands, *Geophys. Res. Lett.23*, 1745-1748, 1996.

Jucks, K. J., D. G. Johnson, K. V. Chance, W. A. Traub, R. J. Salawitch, and R. A. Stachnik, Ozone production and loss rate measurements in the middle stratosphere, *J. Geophys. Res.101*, 28785-28792, 1996.

Jucks, K. J., D. G. Johnson, K. V. Chance, W. A. Traub, J. J. Margitan, G. B. Osterman, R. J. Salawitch, and Y. Sasano, Observations of OH, HO_2, H_2O, and O_3 in the upper stratosphere; Implications for HO_x photochemistry, *Geophys. Res. Lett.25*, 3935–3938, 1998.

Lean, J., M. VanHoosier, G. Brueckner, and D. Prinz, SUSIM/UARS observations of the 120 to 300 nm flux variations during the maximum of the solar cycle: Inferences for the 11-year cycle, *Geophys. Res. Lett.19* 2203-2206, 1992.

Lean, J. L., G. J. Rottman, H. L. Kyle, T. N. Woods, J. R. Hickey, and L. C. Puga, Detection and parameterization of variations in the solar mid and near ultraviolet radiation (200-400 nm), *J. Geophys. Res.102*, 29939-29956, 1997.

Lipson, J. B., et al., Temperature dependence of the rate constant and branching ratio for the OH+ClO reaction, *J. Chem. Soc. Faraday Trans., 93*, 2665-2673, 1997.

Michelsen, H. A., et al., Stratospheric chlorine partitioning: Constraints from shuttle-borne measurements of [HCl], [$ClNO_3$], and [ClO], *Geophys. Res. Lett.23*, 2361-2364, 1996.

Michelsen, H. A., G. L. Manney, M. R. Gunson, C. P. Rinsland, and R. Zander, Correlations of stratospheric [CH_4] and [N_2O] derived from ATMOS measurements made during the ATLAS space shuttle missions, *Geophys. Res. Lett.25*, 2777-2780, 1998a.

Michelsen, H. A., G. L. Manney, M. R. Gunson, and R. Zander, Correlations of stratospheric [NO_y], [O_3], [N_2O], and [CH_4] derived from ATMOS measurements, *J. Geophys. Res.103*, 28347-28359, 1998b.

Minschwaner, K., R. J. Salawitch, and M. B. McElroy, Absorption of solar radiation by O_2: Implications for O_3 and lifetimes of N_2O, $CFCl_3$, and CF_2Cl_2, *J. Geophys. Res.98*, 10543-10561, 1993.

Morris, G. A., D. B. Considine, A. E. Dessler, S. R. Kawa, J. Kumer, J. Mergenthaler, A. Roach, and J. M. Russell III, Nitrogen partitioning in the middle stratosphere as observed by the Upper Atmosphere Research Satellite, *J. Geophys. Res.102*, 8955-8965, 1997.

Osterman, G. B., B. Sen, G. C. Toon, R. J. Salawitch, J. J. Margitan, and J.-F. Blavier, The partitioning of reactive nitrogen species in the summer Arctic stratosphere, *Geophys. Res. Lett.26*, 1157-1160, 1999.

Perrin, A., Recent progress in the analysis of HNO_3 spectra, *Spectrochim. Acta A, 54*, 375-393, 1998.

Salawitch, R. J., et al., The distribution of hydrogen, nitrogen, and chlorine radicals in the lower stratosphere: Implications for changes in O_3 due to emission of NO_y from supersonic aircraft, *Geophys. Res. Lett.21*, 2547-2550, 1994.

Sen, B., et al., Measurements of reactive nitrogen in the stratosphere, *J. Geophys. Res.103*, 3571-3585, 1998.

Thomason, L. W., L. R. Poole, and T. Deshler, A global climatology of stratospheric aerosol surface area density deduced from Stratospheric Aerosol and Gas Experiment II measurements: 1984-1994, *J. Geophys. Res.102*, 8967-8976, 1997.

Volk, C. M., et al., Quantifying transport between the tropical and mid-latitude lower stratosphere, *Science, 272*, 1763-1768, 1996.

Woodbridge, E. L., et al., Estimates of total organic and inorganic chlorine in the lower stratosphere from *in situ* measurements during AASE II, *J. Geophys. Res.100*, 3057-3064, 1995.

World Meteorological Organization (WMO), Atmospheric ozone 1985: Assessment of our understanding of the processes controlling its present distribution and change, *WMO Rep. 16*, Global Ozone Res. and Monit. Proj., Geneva, Switzerland, 1986.

This preprint was prepared with the AGU LaTeX macros v3.1. File hno3 formatted 1999 December 2.